High frequency sound propagation in a network of interconnecting streets

D. P. Hewett [,a,1]

[a]Oxford Centre for Industrial and Applied Mathematics (OCIAM), Mathematical Institute, 24–29 St. Giles, Oxford OX1 3LB, UK

Abstract

We propose a new model for the propagation of acoustic energy from a time-harmonic point source through a network of interconnecting streets in the high frequency regime, in which the wavelength is small compared to typical macro-lengthscales such as street widths/lengths and building heights. Our model, which is based on geometrical acoustics (ray theory), represents the acoustic power flow from the source along any pathway through the network as the integral of a power density over the launch angle of a ray emanating from the source, and takes into account the key phenomena involved in the propagation, namely energy loss by wall absorption, energy redistribution at junctions, and, in 3D, energy loss to the atmosphere. The model predicts strongly anisotropic decay away from the source, with the power flow decaying exponentially in the number of junctions from the source, except along the axial directions of the network, where the decay is algebraic.

Key words: Urban Acoustics, Frequency Domain, High Frequency, Multiple Scattering.

---

1. Introduction

The main difficulties arising in a mathematical study of urban sound propagation are due to the complex geometry of the propagation domain. The presence of multiple scatterers such as buildings, vegetation, vehicles, pedestrians and street furniture, all of which have different acoustical scattering properties, serves to create an extremely complicated sound field, an exact description of which, either analytical or numerical, is usually impossible.

Broadly speaking, the effect of domain complexity occurs on two distinct lengthscales. On the 'microscale' we have the effects of wall absorption, scattering by wall inhomogeneities, and scattering by the obstacles present in each street. On the 'macroscale' we may view an urban environment as a network of streets and junctions, through which acoustic energy propagates.

The existing urban acoustics literature focuses mainly on the modelling of microscale effects, in particular on the accurate prediction of the sound field in a single street. Even in the absence of traffic, pedestrians, vegetation and street furniture this presents a major challenge, because of the

Tel. +44 118 3785012

Email address: d.p.hewett@reading.ac.uk (D. P. Hewett)

[1]Present address: Department of Mathematics, University of Reading, Whiteknights, PO Box 220, Reading RG6 6AX, UK

absorbent and inhomogeneous nature of building facades. A number of different models have been proposed, some based on ray theory [1, 2, 3, 4, 5], others on modal decomposition [6, 7] and others on transport and diffusion approximations [8, 9] - for a more detailed overview see e.g. [10, 11, 12, 13].

The difficulty of the microscale problem has meant that relatively little theoretical work has been published on the macroscale problem of propagation in environments involving multiple streets, and this is the problem we address in this paper. Specifically, we consider the propagation of acoustic energy from a time-harmonic point source in a network of interconnecting streets, in the high frequency regime where the wavelength is small compared to typical macro-lengthscales such as street lengths and widths. In order to facilitate study of the macroscale problem we adopt a rather simple microscale model, in which building facades are assumed to be homogeneous, the scattering effect of obstacles inside streets is neglected, and metereological effects are ignored.

Our objective is to calculate the acoustic power flow down each street in the network. Our method is based on geometrical acoustics (ray theory), with both the interference between ray fields and diffraction effects being neglected. We shall show how the acoustic power flow across a street cross-section can be approximated by an integral over a ray-angle-resolved power density. A key component in our analysis is a careful study of the redistribution of acoustic energy incident at a typical junction between streets. This single-junction problem has been studied previously in [14, 15], the latter work being in the context of modelling sound propagation along office corridors. However, to the best of our knowledge the results of [14, 15] have not been extended to domains involving more than one junction, until now.

The structure of the paper is as follows. §2 reviews the ray-theoretical model of acoustic energy propagation that will be used. §3 applies this model to the case of a single 2D street, and shows that, under certain assumptions, the acoustic power flow across a street cross-section far from the source can be approximated by an integral over a ray-angle-resolved power density. §4 derives similar integral approximations to the power flows out of the exits of a junction between two 2D streets. §5 extends the method to the calculation of power flows along pathways involving multiple junctions. §6 concerns the calculation of the power flows through a network of interconnecting 2D streets, and shows how the problem can be reformulated as a coupled system of partial difference equations, with an exact solution of this system being derived in a special case. §7 demonstrates the applicability of our 2D model to the prediction of sound propagation in a network of 3D corridors, comparing our results to those in [15]. Finally, §8 describes the generalisation of the 2D model to a 3D urban environment.

2. Ray theory and energy propagation

We assume that the propagation is described by a velocity potential $\phi(\mathbf{x};t)$ satisfying

$$\frac{\partial^2}{\partial t^2}\phi(\mathbf{x};t) = c_0^2 \nabla^2 \phi(\mathbf{x};t);$$

where c_0 is the propagation speed, and $\phi(\mathbf{x};t)$ is related to the velocity and pressure perturbations $\mathbf{u}(\mathbf{x};t)$ and $p(\mathbf{x};t)$ in the acoustic approximation by $\mathbf{u}(\mathbf{x};t) = \nabla$

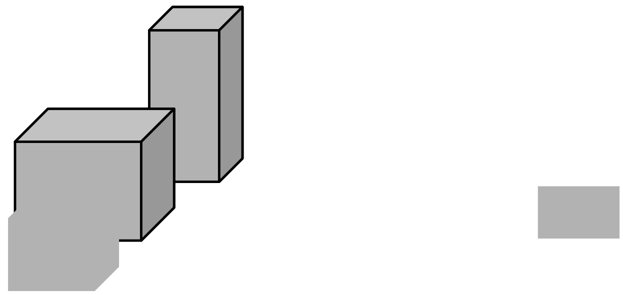

(a) 3D model (b) 2D model

Figure 1: 3D and 2D models of an urban environment.

where $_0$ is the equilibrium density. For time-harmonic waves we assume that $(\mathbf{x}; t) = \mathrm{Re}[(\mathbf{x})e^{i\omega t}]$ for some angular frequency $\omega > 0$. Then, assuming a point source, $(\mathbf{x})$ satisfies the Helmholtz equation

$$(\nabla^2 +$$

a numerical or asymptotic calculation of the full wave solution in one particular realisation of the domain could be achieved, it would be of limited practical relevance [19, 20].

A more robust measure of the broad spatial variation of the sound field can be obtained by studying the distribution of *acoustic energy* across the domain (cf. e.g. [1, 3, 6]) . The acoustic energy and the associated *acoustic intensity* are `quadratic' quantities (i.e. they involve products of two `small' perturbations in the acoustic approximation), which can be averaged both temporally and spatially to provide measures of the magnitude of the sound field that are less sensitive to perturbations in the domain characteristics than are the full details of the wave solution. The *instantaneous acoustic energy density* W and *acoustic intensity* $\mathbf{I}$ are defined by [21]

$$W(\mathbf{x};t) := \frac{1}{2}\rho_0|\mathbf{u}(\mathbf{x};t)|^2 + \frac{1}{2}\frac{(p(\mathbf{x};t))^2}{\rho_0 c_0^2}; \qquad \mathbf{I}(\mathbf{x};t) := p(\mathbf{x};t)\mathbf{u}(\mathbf{x};t); \tag{4}$$

and satisfy the equation of conservation of acoustic energy

$$\frac{\partial W}{\partial t} = -\nabla\cdot\mathbf{I};$$

so that $\mathbf{I}$ describes the instantaneous acoustic energy flux at a given point in space. In the time-harmonic case we remove the temporal oscillations by averaging (4) over one period of oscillation. Denoting the resulting quantities by $\langle W\rangle(\mathbf{x})$ and $\langle\mathbf{I}\rangle(\mathbf{x})$, we find, using (1), that

$$\langle W\rangle(\mathbf{x}) = \frac{\rho_0}{4}\left(\nabla\phi(\mathbf{x})\cdot\overline{\nabla\phi(\mathbf{x})} + k^2\phi(\mathbf{x})\overline{\phi(\mathbf{x})}\right); \qquad \langle\mathbf{I}\rangle(\mathbf{x}) = \frac{\rho_0\omega}{2}\operatorname{Im}[\bar{\phi}(\mathbf{x})\nabla\phi(\mathbf{x})]; \tag{5}$$

where the overbar denotes complex conjugation. The time-averaged acoustic energy flux (or *power flow*) P across a surface 91c DistaTdur[ace1411]T03F1381)Td [( ) 38188 (giv) 27 (en) -333 (b) 28 (y) -333

9J E31 (r) 1 (bar) -3 d 10.9091 Tf 4.7583 14 1 16 [( ) 38n of 'Statistical Energy Analysis' (SEA), a technique used to predict the distribution of vibrational energy in complex mechanical structures (see e.g. [20, 24]). Even in the fully deterministic case, it is sometimes possible to justify the neglect of interference effects by performing some sort of spatial averaging over either the source or receiver location, provided that the averaging region is chosen so that the interference terms oscillate sufficiently to average to zero in the high frequency limit. In [10, §3.5] this statement is verified in the case of a single 2D street, with the averaging region chosen to be a street cross-section. To be precise, in [10] the acoustic power flow down the street is studied, and it is shown that the prediction of the ray model does indeed approximate the exact power flow in the high frequency limit, provided that the source is not too close to either of the street walls and that resonance effects are dealt with appropriately.

The boundary condition (3) assumes that the street walls are perfectly reflecting, and leads to the familiar specular ray reflection law "angle of incidence equals angle of reflection". In practice, some energy incident on the walls is absorbed, and the simplest way of including this in the ray model (cf. [1, 4]) is to introduce an *absorption coefficient* $\alpha \in [0,1]$, such that the magnitude I of the intensity along a ray undergoing a reflection at the boundary is attenuated according to the rule

$$I_{\text{reflected}} = (1-\alpha)\, I_{\text{incident}}.$$

As a first approximation, we take α to be independent of the angle of incidence/reflection. The relationship between this simple ray-based absorption model and full wave-based models such as impedance boundary conditions is rather subtle (see e.g. [25, 26, 27, 28]), and will not be discussed here. However, we remark that the form of the integral approximations derived in this paper would make generalisation to angle-dependent absorption coefficients a possibilit34(to)-33de hmakemakalong aos3/iliv5 T

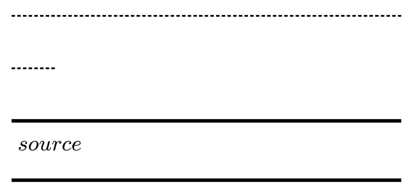

Figure 2: Association between image sources and rays in a single 2D street.

constructed by the method of images. Introducing an infinite array of image sources at the points $(0, y_n)$, $n \in \mathbb{Z} \setminus \{0\}$, where

$$y_n = \begin{cases} n + y_0, & n \text{ even}, n \neq 0, \\ n + (1 - y_0), & n \text{ odd}, \end{cases} \tag{10}$$

a formal solution of (8) satisfying the boundary conditions (9) can be obtained by setting

$$\phi(x, y) = \sum_{n \in \mathbb{Z}} \phi_n(x, y), \tag{11}$$

where $\phi_n(x, y)$ is the free space velocity potential associated with each of the image sources,

$$\phi_n(x, y) = -A \frac{i}{4} H_0^{(1)}\left(k\sqrt{x^2 + (y - y_n)^2}\right).$$

The sum (11) is convergent whenever $k \notin \pi\mathbb{N}$, i.e. away from resonance.

The geometrical acoustics approximation is an infinite sum of ray fields, each being the far-field approximation of the Hankel function associated with one of the image sources. As Figure 2 illustrates, the contribution of each image source $(0, y_n)$ can be associated with exactly one ray emanating from the physical source, with launch angle θ_n given by

$$\theta_n(x, y) = \begin{cases} \operatorname{sgn}(n)(-1)^n \arctan\left(\frac{y_n - y}{x}\right), & n \neq 0, \\ \arctan\left(\frac{y_0 - y}{x}\right), & n = 0. \end{cases}$$

According to the ray model, the acoustic power flow P across a street cross-section at distance x from the source is equal to the incoherent sum of the free space power flows across the street cross-section from each of the image sources. As a fraction of the total free space power output of the source (we shall adopt this normalisation for the remainder of the paper), the power flow from the nth image source is equal to $1/(2\pi)$ times the angular width $\Delta\theta_n = \Delta\theta_n(x, y_0)$ of the tube of rays from the image source that intersect the street cross-section at x (see Figure 3(a)), and

$$P(x) = \frac{1}{2\pi} \sum_{n \in \mathbb{Z}} (1 - \alpha)^{|n|} \Delta\theta_n. \tag{12}$$

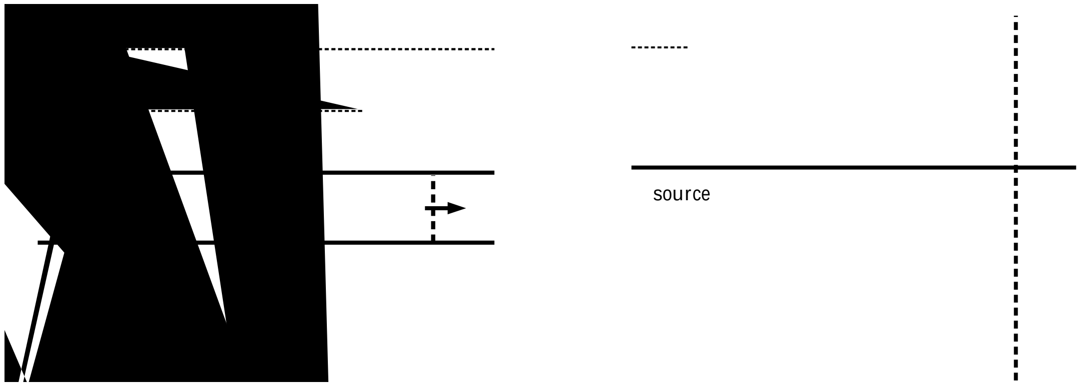

(a) Image sources (b) Image streets

Figure 3: The geometrical interpretation of $_n$ and $\tilde{}_n$ in a single 2D street.

It is convenient to rewrite (12) as

$$P(x) = \frac{1}{2}\sum_{n\in\mathbb{Z}}(1\quad)^{|n|}\,\tilde{}_n; \tag{13}$$

where

$$\tilde{}_n = \begin{cases} \ _n; & n \text{ even};\\ \ _n; & n \text{ odd}. \end{cases} \tag{14}$$

Explicitly, $\tilde{}_n = \tilde{}^+_n \quad \tilde{}_n$, where

$$\tilde{}^+_n = \arctan\frac{n+1\quad y_0}{x}; \qquad \tilde{}_n = \arctan\frac{n\ y}{x}:$$

absorption coe cient. When $1{=}x$, the main contribution to the sum comes from near $n = 0$, and [10, x3.5.2]

$$P(x) \quad \frac{2}{2 \quad x} \quad 1 + \frac{1}{x^2} \quad y_0(1 \quad y_0) \quad \frac{1}{3} \quad \frac{2(1 \qquad)}{2} \quad + O \quad \frac{1}{x^4} \quad ; \quad x \;!\; 1; \qquad 1{=}x: \tag{17}$$

To deal with the case $= O(1{=}x)$, we rst use the identity

$$\arctan z_1 \quad \arctan z_2 = \arctan \frac{z_1 \quad z_2}{1 \quad z_1 z_2} \tag{18}$$

to deduce that

$$\tilde{}_n = \arctan \frac{1}{x + \frac{(n+1 \quad y_0)(n \quad y_0)}{x}} \qquad \frac{1}{x + \frac{n^2}{x}} \quad 1 + O \quad \frac{1}{x} \quad ; \quad x \;!\; 1; \tag{19}$$

uniformly for all n. Inserting (19) into (13) then gives

$$P(x) \quad \frac{1}{2} \qquad \frac{1}{x}$$

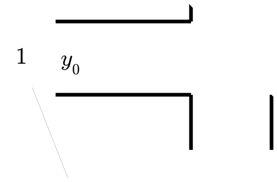

(a) Crossroads

(b) Side street

(c) T-junction

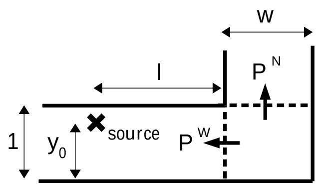

(d) Right-angled bend

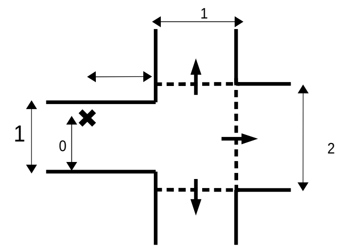

(e) Asymmetric crossroads (

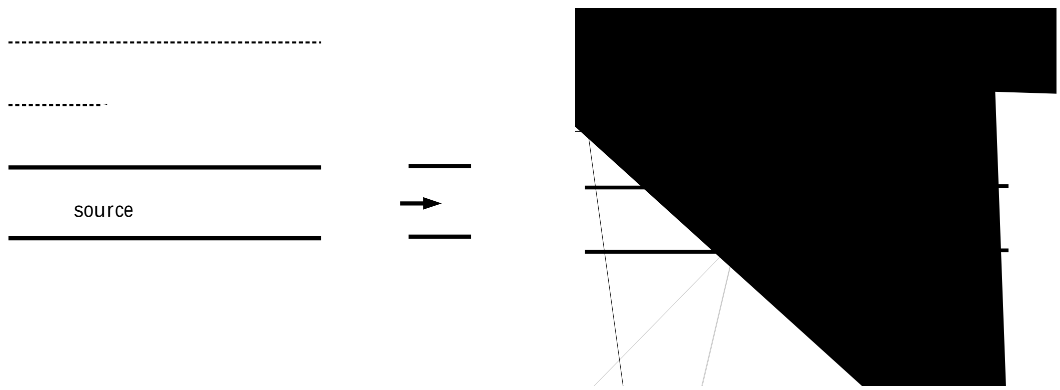

(a) Image sources

(b) Image streets

Figure 5: The geometrical interpretation of $_n$ and $\tilde{}_n$ at a crossroads.

The power ow P^E out of the East exit of the junction is then computed by incoherently summing the power ows along the ray tubes reaching the exit from each of the image sources de ned in (10), so that

$$P^E = \frac{1}{2}\sum_{n \in Z}(1 \quad)^{|n|} \quad {}_n; \tag{23}$$

where is the absorption coe cient of the street containing the source and $_n = \ _n(l; w/l+w$/F15 10.9091 Tf 5.314

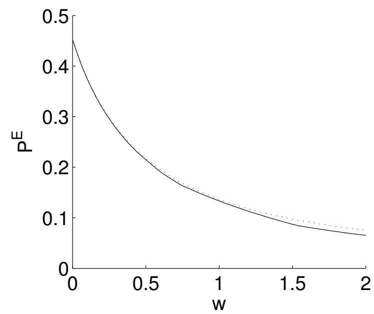

Figure 6: Comparison of ray tube sum (24) (solid line) and the corresponding integral approximation (27) (dotted line) for the power flow past a crossroads, plotted against the side street width w. Here $l = 2$, $y_0 = 0.3$, $\epsilon = 0.02$.

Inserting (26) into (24) and approximating the sum by an integral, we find that

$$P^E \approx \frac{1}{\pi}\int_0^{1/w}(1-\epsilon)^{lt}\frac{1-wt}{1+t^2}\,dt + O\left(\frac{1}{l}\right); \quad l \to \infty;\ w = O(1); \quad \epsilon = O(1/l). \qquad (27)$$

a crossroads of side street width $2w$, so that

$$P^W \quad \frac{1}{} \int_0^{=2} (1 \quad)^{l \tan} F_C(\; ; 2w)\, d \; ; \qquad P^N \quad P^S \quad \frac{1}{} \int_0^{=2} (1 \quad)^{l \tan} F_T(\; ; 2w)\, d \; ;$$

where P^W should be interpreted as the power ow back down the main street due to re ection o the far wall. Power ows in the `right-angled bend' geometry of Figure 4(d) can be treated similarly.

Asymmetric junctions such as those in Figures 4(e) and 4(f) can alsoWAl(thuigh)]TJ 0 -13.549 Td [(suc)28(h)-6
$F_C($;
2Werpreaction in Figure 4(e (,)-50[(where)]TJ/F39 10.9091 Tf297.2909 0 Td [wl
that-2239(the)-228(oseat-2239(and)2239or)1(iee)-1inaction ft-2239(n)-228radthe junctiot-2239(ren)-228random(,)2

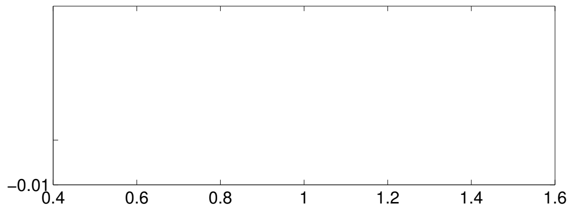

(a) $I_0 = 20$

(b) $I_0 = 100$

Figure 10: Plot of the error $R = P$

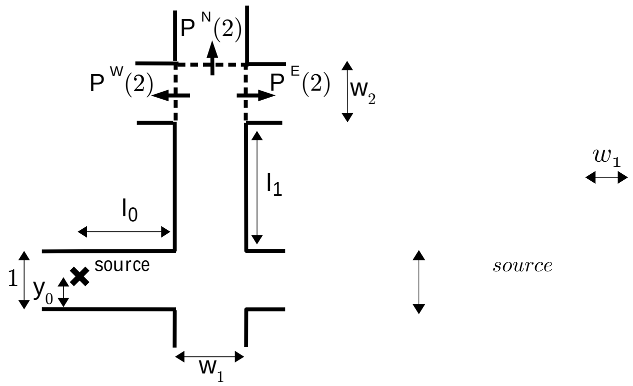

(a) Another two-junction geometry

(b) A three-junction geometry

Figure 12: Multiple-junction geometries

5.3. *Further examples*

The case where the absorption coe cient takes a value $_0$ between the source and the rst junction, and a di erent value $_1$ between the rst and second junctions, can be treated by modifying (36) to

$$P^E_{\text{app}}(2) = \frac{1}{\ } \mathrm{Z}_0^{\ =2} (1 \quad _0)^{l_0 \tan} \; F_C(\ ; w_1)\,(1 \quad _1)^{l_1 \tan} \; F_C(\ ; w_2)\, d\ : \tag{38}$$

Expected values of $P^N(2)$ and $P^S(2)$ can be obtained by replacing the factor of $F_C(\ ; w_2)$ in (38) by a factor of $F_T(\ ; w_2)$, so that

$$P^N_{\text{app}}(2) = P^S_{\text{app}}(2) = \frac{1}{\ } \mathrm{Z}_0^{\ =2} (1 \quad _0)^{l_0 \tan} \; F_C(\ ; w_1)\,(1 \quad _1)^{l_1 \tan} \; F_T(\ ; w_2)\, d\ :$$

In Figure 12(a) we consider another two-junction geometry. The integral approximations we propose for the expected power ows out of the second junction are

$$P^N_{\text{app}}(2) = \frac{1}{\ } \mathrm{Z}_0^{\ =2} (1 \quad _0)^{l_0 \tan} \; F_T(\ ; w_1)\,(1 \quad _1)^{\frac{l_1}{w_1} \tan (\ =2 \quad)} F_C \quad =2 \quad ; \frac{w_2}{w_1} \quad d\ ; \tag{39}$$

$$P^E_{\text{app}}(2) = P^W_{\text{app}}(2) = \frac{1}{\ } \mathrm{Z}_0^{\ =2} (1 \quad _0)^{l_0 \tan} \; F_T(\ ; w_1)\,(1 \quad _1)^{\frac{l_1}{w_1} \tan (\ =2 \quad)} F_T \quad =2 \quad ; \frac{w_2}{\ }$$

5.4. More than two junctions

Integral approximations for the expected power flows in domains involving more than two junctions can be constructed similarly. For example, consider the path shown in Figure 12(b). For generality, the street width w_0 is assumed to be of the same order of magnitude, but not the exactly equal to, the characteristic lengthscale L used in the nondimensionalisation. We then approximate $P^N(3)$ by

$$P^N_{\text{app}}(3) = \frac{1}{\pi}\int_0^{\pi/2} (1-\mu_0)^{\frac{l_0}{w_0}\tan\theta} F_C\left(\theta;\frac{w_1}{w_0}\right)(1-\mu_1)^{\frac{l_1}{w_0}\tan\theta} F_T\left(\theta;\frac{w_2}{w_0}\right)$$
$$(1-\mu_2)^{\frac{l_2}{w_2}\tan(\pi/2-\theta)} F_C\left(\pi/2-\theta;\frac{w_3}{w_2}\right) d\theta .$$

Since $F_C(\theta;w_1/w_0)$ vanishes for $\theta \geq \arctan(w_0/w_1)$, and $F_R(\pi/2-\theta;w_3/w_2)$ vanishes for $\theta \leq \arctan(w_3/w_2)$, we find that if $w_3/w_2 \geq w_0/w_1$ then the expected power flow is zero, since the integrand vanishes completely on the range $(0,\pi/2)$.

This example illustrates a more general result. Suppose that an arbitrary path through a network of streets crosses a junction in the East-West direction, with the ratio between the widths of the `side street' and the `main street' given by R_{EW}, and that this path also crosses a junction in the North-South direction, with the ratio between the widths of the `side street' and the `main street' given by R_{NS}. Then if $R_{EW}R_{NS} \geq 1$, the expected power flow along the path is zero. In particular, in the special case where the street widths are all equal, there is no expected power flow along any path which crosses junctions in both the East-West and North-South directions.

6. A network of streets in 2D

We now apply the ideas developed in §3-5 to estimate the power flows in an infinite rectangular network of streets intersecting at right-angled crossroads. Indexing the crossroads by $(x,y) \in \mathbb{Z}\times\mathbb{Z}$, we let $l^S_{x,y}, w^S_{x,y}, \mu^S_{x,y}$ and $l^W_{x,y}, w^W_{x,y}, \mu^W_{x,y}$ denote the lengths, widths and absorption coefficients of the streets to the South and West respectively of junction (x,y). We assume that the source lies in the street between junctions $(0,0)$ and $(1,0)$, a distance d_0 from the junction $(1,0)$.

The net power flows $P^N_{x,y}$, $P^E_{x,y}$, $P^S_{x,y}$ and $P^W_{x,y}$ out of a junction (x,y) are made up of contributions from the infinitely many propagation paths that exist between the source and that junction. The expected power flow along any particular path can be estimated by the integral approximation method developed in §3-5, provided that the street lengths are much larger than the street widths, and that the absorption coefficients are small. Some paths make a positive contribution to the power flow, and others make a negative one, depending on the direction in which the energy is propagating when it crosses the junction exit in question. Some paths make no contribution at all, as remarked in §5.4. Classifying all of these paths and explicitly summing their respective contributions might appear to be rather difficult, but in §6.2 we show how this can be achieved by reformulating the problem as a coupled system of partial difference equations. Before describing this model, we first show how an approximation to the net power flows can be obtained by considering a subset of paths which make the largest contribution. To demonstrate this, we consider the special case of a *regular* network in which $l^S_{x,y} = l^W_{x,y} = l$, $w^S_{x,y} = w^W_{x,y} = w$ and $\mu^S_{x,y} = \mu^W_{x,y} = \mu$ for all (x,y), where l, w and μ are constant. Furthermore we assume, without loss of generality, that $x \geq 1$ and $y \geq 0$, and study the net power flow $P^E_{x,y}$ out of the East exit of the junction (x,y).

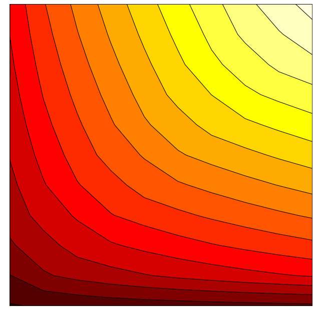

(a) = 0:9 (b) = 0:4

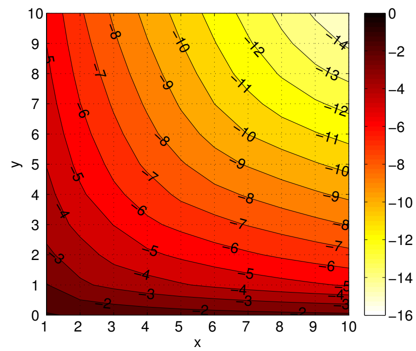

(c) = 0:9 (d) = 0:4

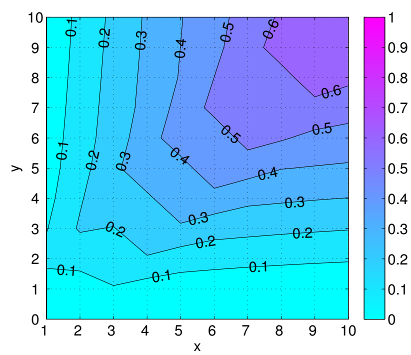

(e) = 0:9 (f) = 0:4

Figure 13: (a)-(b) Contour plots of $\log_{10} P^E_{x;y}$ for two di erent values of , computed by (41) (i.e. using only paths of minimal length). (c)-(d) Corresponding plots of $\log_{10} P^E_{x;y}$, computed by (52) (i.e. by solving the full partial di erence equation model). (e)-(f) Relative error between the two.

which is a Laplace-type integral with large parameter N. The main contribution to (43) comes from the left endpoint = 0, and a local expansion around this point reveals that

$$P_0^E(N) \sim \frac{1}{N}; \quad N \to \infty; \tag{44}$$

so that the decay is *algebraic* in the number of junctions encountered.

Along the diagonal = 1=2 (with N even) there is again only one contributing path of minimal length ($M_{1=2}(N) = 1$ for all N even) and our estimate for $P^{E}_{1=2}(N)$ is

$$P^{E}_{1=2}(N) = \frac{1}{}\int_{0}^{=2} F_T(\;;1)^{N=2}\, F_T(\;=2\quad;1)^{N=2}\, d\quad = \frac{2}{}\int_{0}^{=4} \exp\; N\;\; \frac{1}{2}\log\;\frac{\tan}{4}\quad d\;;$$

where we have used the symmetry of the integrand to reduce the range of integration to $2\ (0;\ =4)$. Again, this is a Laplace-type integral, although this time the main contribution comes from the right endpoint $\ =\ =4$, with

$$P^{E}_{1=2}(N)\quad \frac{2}{N}\quad \frac{1}{2}^{\;N}; \qquad N\ !\ 1;\ N \text{ even}; \tag{45}$$

so that the decay is *exponential* in the number of junctions encountered.

) 2 , 9 10.9091 Tf 7.273 0 Td

In the intermediate case $0 < \ < 1=2$, we rst note that by Stirling's approximation,

$$M\ (N) = \frac{((1\quad)N)!}{(\;N)!((1\quad 2\;)N)!}\qquad s\,\frac{(1\quad)}{2\;N\;(1\quad 2\;)}\;)$$

6.2. Partial di erence equation model

So far we have considered only the contribution from paths of minimal length. We now generalise our model to take into account the contribution of *all* the propagation paths through the network. At each junction in the lattice we de ne $p^N_{x;y}(\ );\ p^E_{x;y}(\ );\ p^S_{x;y}(\ );\ p^W_{x;y}(\ )$ to be the -resolved power ows out of the junction $(x;y)$ in the North, East, South and West directions, respectively. We can use the energy redistribution and absorption rules suggested by the integral approximations developed in previous sections to write down a coupled system of partial di erence equations satis ed by these quantities. For example, the power ow $p^N_{x;y}(\ )$ out of the North exit is a sum of contributions owing in from the East, South and West streets, each involving an appropriate choice of the redistribution functions F_C and F_T. The resulting system of partial di erence equations, for the case of a general network of streets, is

$$\begin{aligned}
p^N_{x;y} &= F_C \quad =2 \quad ; \frac{w^W_{x;y}}{w^S_{x;y}} \quad (\ ^N_{x;y\ \ 1})^{1=t} p^N_{x;y\ \ 1} + F_T \quad ; \frac{w^S_{x;y}}{w^W_{x;y}} \quad (\ ^E_{x\ \ 1;y})^t p^E_{x\ \ 1;y} + (\ ^W_{x+1;y})^t p^W_{x+1;y} \ + \ \ ^N_{x;y};\\
p^E_{x;y} &= F_C \quad ; \frac{w^S_{x;y}}{w^W_{x;y}} \quad (\ ^E_{x\ \ 1;y})^t p^E_{x\ \ 1;y} + F_T \quad =2 \quad ; \frac{w^W_{x;y}}{w^S_{x;y}} \quad (\ ^N_{x;y\ \ 1})^{1=t} p^N_{x;y\ \ 1} + (\ ^S_{x;y+1})^{1=t} p^S_{x;y+1} \ + \ \ ^E_{x;y};\\
p^S_{x;y} &= F_C \quad =2 \quad ; \frac{w^W_{x;y}}{w^S_{x;y}} \quad (\ ^S_{x;y+1})^{1=t} p^S_{x;y+1} + F_T \quad ; \frac{w^S_{x;y}}{w^W_{x;y}} \quad (\ ^E_{x\ \ 1;y})^t p^E_{x\ \ 1;y} + (\ ^W_{x+1;y})^t p^W_{x+1;y} \ + \ \ ^S_{x;y};\\
p^W_{x;y} &= F_C \quad ; \frac{w^S_{x;y}}{w^W_{x;y}} \quad (\ ^W_{x+1;y})^t p^W_{x+1;y} + F_T \quad =2 \quad ; \frac{w^W_{x;y}}{w^S_{x;y}} \quad (\ ^N_{x;y\ \ 1})^{1=t} p^N_{x;y\ \ 1} + (\ ^S_{x;y+1})^{1=t} p^S_{x;y+1} \ + \ \ ^W_{x;y};
\end{aligned} \tag{50}$$

where $t = \tan$,

$$\begin{aligned}
&{}^S_{x;y} = (1 \quad {}^S_{x;y})^{\frac{l^S_{x;y}}{w^S_{x;y}}}; &\qquad &{}^W_{x;y} = (1 \quad {}^W_{x;y})^{\frac{l^W_{x;y}}{w^W_{x;y}}};\\
&{}^N_{x;y} = \ {}^S_{x;y+1}; &\qquad &{}^E_{x;y} = \ {}^W_{x+1;y};
\end{aligned}$$

and ^{N}, ^{E} ^{S} and ^{W} are source terms to be speci ed according to the distribution of sources in the network. For example, in the case where the source lies in the street between junctions $(0;0)$ and $(1;0)$, theS

Furthermore, knowledge of the -resolved power densities also allows us to calculate the average

With p^N determined by (57) and (60), the remaining variables $p^E; p^S$ and p^W can be expressed in terms of p^N as follows:

$$p^S = p^N + (\;{}^S \quad {}^N); \tag{61}$$

$$p^E = \;1 \quad X^{\;1}\;\;^{1} \; \frac{1{=}t}{2} \; (Y + Y^{\;1})p^N + Y(\;{}^S \quad {}^N) \; + \;{}^E \; ; \tag{62}$$

$$p^W = [1 \quad X]^{\;1} \; \frac{1{=}t}{2} \; (Y + Y^{\;1})p^N + Y(\;{}^S \quad {}^N) \; + \;{}^W \; : \tag{63}$$

The inverse operators $1 \quad X^{\;1}\;\;^{1}$ in (62) and (63) are given formally by the sums

$$1 \quad X^{\;1}\;\;^{1} = \sum_{n=0}^{1} (\; X^{\;1})^n$$

and the source functions are zero everywhere except for

$$ {}^{N}_{0;0} = {}^{S}_{0;0} = \frac{(l \quad d)t}{l} \quad \frac{1}{2} \quad ; \qquad {}^{N}_{1;0} = {}^{S}_{1;0} = \frac{dt}{l} \quad \frac{1}{2} \quad : \tag{67} $$

Noting that (66) is simply (54) with

$$ N \leftrightarrow E; \qquad S \leftrightarrow W; \qquad t \leftrightarrow 1/t; \qquad X \leftrightarrow Y; \tag{68} $$

the solution of (66), valid for $/4 < \quad < /2$, is found to be

$$ \begin{aligned} p^N &= \tilde{\ } \quad \bar{H}^+ + \bar{S}_1; \qquad & p^E &= \tilde{\ } \quad \bar{G}; \\ p^S &= \tilde{\ } \quad \bar{H} \quad + \bar{S}_3; \qquad & p^W &= \tilde{\ } \quad \bar{G} + \bar{S}_2; \end{aligned} \tag{69} $$

where $\tilde{\ }$ and $\bar{S}_i$ are the previously defined expressions and S_i under the transformations (68), and

$$ \bar{G}_{x;y} = G_{y;x}; \qquad \bar{H}_{x;y} = H_{y;x}; $$

under the transformation $t \leftrightarrow 1/t$. From (67) we find that $\tilde{\ }$ is zero everywhere except for

$$ \begin{aligned} \tilde{\ }_{0;0} &= \frac{1}{2}\frac{t}{t} \quad 1/t + \frac{(l \quad d)t}{l}; \qquad & \tilde{\ }_{1;0} &= \frac{1}{2}\frac{t}{t} \quad 1/t + \frac{dt}{l}; \\ \tilde{\ }_{0;\ 1} = \tilde{\ }_{0;1} &= \frac{1}{4} \quad \frac{(l \quad d)t}{l}; \qquad & \tilde{\ }_{1;\ 1} = \tilde{\ }_{1;1} &= \frac{1}{4} \quad \frac{dt}{l}: \end{aligned} $$

In Figure 13(c)-(d) we show logarithmic plots of the net power flow P^E defined by (52), computed using the solutions (65) and (69), for two different values of . Comparing these to Figure 13(a)-(b) we note that the anisotropic decay predicted by the minimal length paths approach is clearly visible, although, as might have been expected, the minimal length path calculation underestimates the power flow derived via the full partial difference equation model. The relative error between (41) and (52) is plotted in Figure 13(e)-(f). Note that the relative error decreases as decreases, so that the contribution of the non-minimal-length paths becomes less important as the amount of absorption increases.

As remarked in §6.3, knowledge of the power densities $p^N_{x;y}(\ ); p^E_{x;y}(\ ); p^S_{x;y}(\ ); p^W_{x;y}(\ )$ also allows us to estimate average energy densities and mean-square pressures. In Figure 14 we show logarithmic plots of the average energy density W^E defined by (53) for two different values of .

6.5. The case $= 1$ ($= 0$)

When $= 1$ ($= 0$) the integral (59) is no longer convergent, and the -resolved power flows are no longer well-defined. However, we note that it is still possible to compute net power flows such as (52) by considering the limiting value of the net power flow as $\to 1$, which is well-defined because the singularities in $p^E_{x;y}$ and $p^W_{x;y+1}$ for $= 1$ exactly cancel.

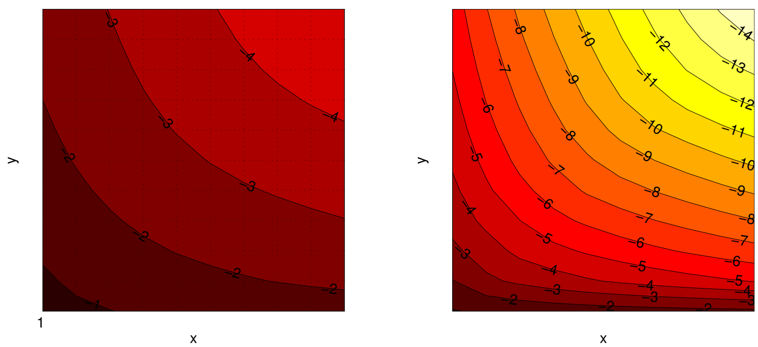

(a) = 0:9 (b) = 0:4

Figure 14: Contour plots of $\log_{10} W^{E}_{x;y}$

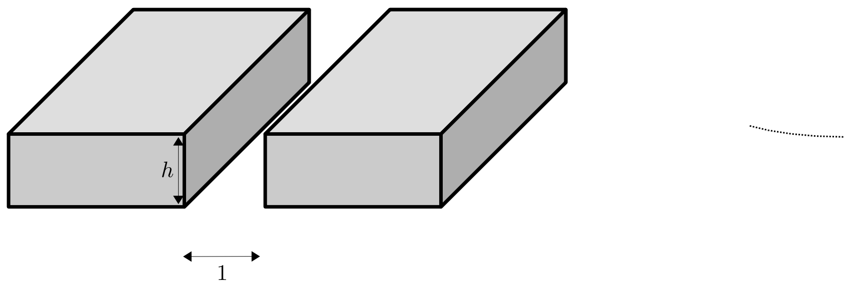

(a) Problem geometry and image source configuration (b) Projection onto the unit sphere

Figure 15: A single street in 3D

8. A 3D urban environment

We now discuss the generalisation of the results of the preceding sections to 3D urban environments. The main ways in which the 3D problem differs from the 2D case are the higher rate of geometrical spreading, the presence of a ground reflection, and the fact that energy emitted from the source can escape to the atmosphere.

8.1. Ray approximation in a single street

As a simple model of a single street in 3D, we consider an infinitely-long channel running parallel to the x-axis, as illustrated in Figure 15(a). After nondimensionalising lengths by the street width, the street is bounded by buildings $(-\infty,\infty)\times(-\infty,0)\times(0,h)$ and $(-\infty,\infty)\times(1,\infty)\times(0,h)$, where $h>0$ is the (nondimensional) building height, assumed constant along the length of the street, and a rigid ground $(-\infty,\infty)\times(0,1)\times\{0\}$. We assume that a point source is located within the street at $(0,y_0,z_0)$, where $0<y_0<1$ and $0<z_0<h$.

As in the 2D case, we simplify the analysis by neglecting the effects of diffraction, and consider the contribution of the multiply-reflected field alone. This can be computed by the introduction of image sources at the points $(0,y_n,\pm z_0)$, $n\in\mathbb{Z}$, with y_n defined as in (10) (see Figure 15(a)). We note that although a ray can undergo an arbitrarily large number of reflections in the walls of the street, no ray undergoes more than one ground reflection. The field is then approximated by

$$\frac{1}{4\pi}\sum_{z\in\mathbb{Z}}\left(\frac{e^{ikr_n}}{r_n}+\frac{e^{ikr_n^+}}{r_n^+}\right), \tag{72}$$

where $r_n^{\pm}=\sqrt{x^2+(y-y_n)^2+(z\mp z_0)^2}$. For simplicity we consider only the case where the source is close enough to the ground to ensure that the interference between each image source and its corresponding ground-reflected image source in (72) is entirely constructive (the general case would require a more careful treatment of the ground reflection, and will not be considered here). Each pair of image sources at $(0,y_n,\pm z_0)$ can then be replaced by a single image source at $(0,y_n,0)$ of double the amplitude (four times the power output), so that

$$\frac{1}{2}\sum_{z\in\mathbf{Z}}\frac{e^{ikr_n}}{r_n}, \tag{73}$$

where $r_n = \sqrt{x^2 + (y - y_n)^2 + z^2}$. It is shown in [10, §3.9.1] that for (73) to hold it is sufficient to assume that $x \gg 1/k$ (so we are not too close to the source) and that $z_0 \ll x/(kh)$.

8.2. The acoustic power flow in a single street

As in the 2D case, we assume that the intensity contributions from the infinitely many image sources in (73) can be summed incoherently, with the effect of interference being neglected. The power flow P across the street cross-section $\{x\} \times (0,1) \times (0,h)$, as a fraction of the total free space power output of the source, is then

$$P = \frac{1}{4\pi}\sum_n (1-\alpha)^{|n|}\tilde{\Omega}_n, \tag{74}$$

where α is the absorption coefficient of the walls and $\tilde{\Omega}_n$ is the solid angle subtended at the source by the ray tube incident on the

(a) Problem geometry

(b) the functions E_{3D} (solid) and E_{2D} (dotted)

Figure 16: A crossroads in 3D.

where the absorption factor $A(\ )$ and the energy redistribution factor $F(\ )$ are exactly as in the analogous 2D problem. We expect (82) to provide a good approximation to (79) only when the streets in the network are long and the typical absorption coe cient is small. Furthermore, when multiple junctions are involved, we conjecture, as in the 2D case, that the approximations represent *expected* power ows after averaging over a suitable range of street lengths. Note that when also $L(\ ) \quad h$

By comparison with (76), we see that the prefactor $2h/(\pi l)$ in (84) represents the power incident on the junction. Thus the fraction E_{3D} of energy incident on the junction that carries on down the main street is given as a function of w by

$$E_{3D}(w) = \int_0^{\pi/2} F_C(\theta; w)\cos\theta \, d\theta \, .$$

The corresponding expression in 2D is

$$E_{2D}(w) = \frac{2}{\pi}\int_0^{\pi/2} F_C(\theta; w)\, d\theta \, .$$

A plot of the functions E_{2D} and E_{3D} is presented in Figure 16(b). Note that in 3D a greater proportion of the incident energy passes the junction than in 2D. This is because in 3D the energy incident on the junction is not distributed uniformly over all $\theta \in (0, \pi/2)$, as it is in the two dimensional case; rather there is a bias towards rays with small θ, as remarked at the end of §8.2 (and see Figure 15(b)). Such rays contribute more to the power flow than those with larger θ because $F_C(\theta; w)$ is a decreasing function of θ.

8.5. A two-junction environment

As a further example, we consider the 3D analogue of the 2D two-junction environment illustrated in Figure 12(a), for which the approximations (39) and (40) were obtained. In the 3D case the integral approximation (82) of the power flows $P^E(2)$ and $P^W(2)$ would have

$$A(\theta) = (1-\alpha_0)^{l_0 \tan\theta}(1-\alpha_1)^{\frac{l_1}{w_1}\tan(\pi/2-\theta)}, \tag{85}$$

$$F(\theta) = F_T(\theta; w_1)F$$

When $\quad = 0$ we have

$$F(\ ) = F_C(\ ;1)^N; \qquad L(\ ) = \frac{Nl}{\cos};$$

and our estimate for $P_0^E(N)$ is

$$P_0^E(N) = \frac{2h}{Nl}\int_0^{\ =4} \exp\left[N \log(1 \quad \tan \ )\right]\cos \ d\ :$$

We nd that

$$P_0^E(N) \quad \frac{2h}{N^2 l}; \qquad N \to \infty;$$

so that the decay is *algebraic* in the number of junctions encountered.

Along the diagonal $\quad = 1{=}2$ (with N even) we have

$$F(\ ) = F_C(\ ;1)^{N=2} F_T(\ =2 \quad ;1)^{N=2}; \qquad L(\ ) = \frac{Nl}{2}\quad \frac{1}{\cos} + \frac{1}{\sin} \quad ;$$

and our estimate for $P_{1=2}^E(N)$ is

$$P_{1=2}^E(N) = \frac{8h}{Nl}\int_0^{\ =4} \exp\quad N \quad \frac{1}{2}\log \quad \frac{\tan}{4} \qquad \frac{1}{\frac{1}{\cos} + \frac{1}{\sin}}\, d\ :$$

We nd that

$$P_{1=2}^E(N) \quad \frac{2\sqrt{2}h}{N^2 l} \quad \frac{1}{2}^{\ N}; \qquad N \to \infty;\ (N \text{ even});$$

so that the decay is *exponential* in the number of junctions encountered.

It is not clear whether the integral approximations derived here can be used to formulate a partial di erence equation model analogous to that proposed for the 2D case in §6.2. There we were able to relate the -resolved power ows into one junction to the -resolved power ows out of the neighbouring junctions. This formulation relies crucially on the fact that the absorption and energy pathway through the network as the integral of a power density over the launch angle of a ray emanating from the source. The dependence of the power density on the launch angle takes into account the key phenomena involved in the propagation, namely energy loss by wall absorption, energy redistribution at junctions, and, in 3D, energy loss to the atmosphere. We have shown, by means of a number of examples, how the power density for a given propagation pathway may be explicitly computed.

Computing the total net power flow across a street cross-section requires the summation of the power flows along each of propagation pathways from the source. An estimate can be obtained by considering only paths of minimal length. In 2D the full summation can be computed implicitly, by formulating a system of partial difference equations for the power densities flowing out of the exits of each junction in the network. In a special case we were able to obtain an exact solution to this system. However, the generalisation of this formulation to the 3D case remains an area for future research.

In summary, our model predicts strongly anisotropic decay away from the source, with the power flow decaying exponentially in the number of junctions from the source, except along the axial directions of the network, where the decay is algebraic. The model is not only concerned with the calculation of acoustic power flows - once the power density has been determined, an elementary modification of the integral allows us to compute the acoustic energy density and the mean-square pressure, averaged over the street cross-section.

10. Acknowledgements

The author would like to thank Prof. J. R. Ockendon, Dr D. J. Allwright and Prof. C. J. Chapman for their helpful comments, and gratefully acknowledges the support of the EPSRC and Dstl (MOD research programme, contract RD023-2985).

References

[1] F. M. Wiener, C. I. Malme, C. M. Gogos, Sound propagation in urban areas, J. Acoust. Soc. Am. 37 (4) (1965) 638–747.

[2] R. H. Lyon, Role of multiple reflections and reverberation in urban noise propagation, J. Acoust. Soc. Am. 55 (3) (1974) 493–503.

[3] H. G. Davies, Multiple-reflection diffuse-scattering model for noise propagation in streets, J. Acoust. Soc. Am. 64 (2) (1978) 517–521.

[4] K. K. Iu, K. M. Li, The propagation of sound in narrow street canyons, J. Acoust. Soc. Am. 112 (2) (2002) 537–550.

[5] J. Kang, Sound propagation in street canyons: comparison between diffusely and geometrically reflecting boundaries, J. Acoust. Soc. Am. 107 (2000) 1394–1404.

[6] R. Bullen, F. Fricke, Sound propagation in a street, J. Sound Vib. 46 (1) (1976) 33–42.

[7] A. Pelat, S. Felix, V. Pagneux, On the use of leaky modes in open waveguides for the sound propagation modeling in street canyons, J. Acoust. Soc. Am. 126 (2009) 2864{2872.

[8] J. Picaut, L. Simon, J. Hardy, Sound eld modelling in streets with a di usion equation, J. Acoust. Soc. Am. 106 (5) (1999) 2638{2645.

[9] T. Le Polles, J. Picaut, M. Berengier, C. Bardos, Sound eld modeling in a street canyon with partially di usely re ecting boundaries by the transport theory, J. Acoust. Soc. Am. 116 (5) (2004) 2969{2983.

[10] D. P. Hewett, Sound propagation in an urban environment, DPhil thesis, University of Oxford, 2010.

[11] J. Kang, Urban Sound Environment, Taylor and Francis, 2006.

[12] R. H. Lyon, Propagation of environmental noise, Science 179 (1973) 1083{1090.

[13] K. Attenborough, K. M. Li, K. Horoshenkov, Predicting Outdoor Sound, Taylor and Francis, 2006.

[14] R. Bullen, F. Fricke, Sound propagation at a street intersection in an urban environment, J. Sound Vib. 54 (1) (1977) 123{129.

[15] H. G. Davies, Noise propagation in corridors, J. Acoust. Soc. Am. 53 (5) (1973) 1253{1262.

[16] M. Crocker, Handbook of Noise and Vibration Control, John Wiley and Sons, 2007.

[17] J. B. Keller, Geometrical theory of di raction, J. Opt. Soc. Am. 52 (2) (1962) 116{130.

[18] V. A. Borovikov, B. Y. Kinber, Geometrical Theory of Di raction, The Institution of Electrical Engineers, 1994.

[19] F. Fahy, Sound Intensity, Taylor and Francis, 1995.

[20] C. H. Hodges, J. Woodhouse, Theories of noise and vibration transmission in complex structures, Rep. Prog. Phys. 49 (1986) 107{170.

[21] M. J. Lighthill, Waves in Fluids, Cambridge University Press, 2003.

[22] A. G. Galitsis, W. N. Patterson, Prediction of noise distribution in various enclosures from free- eld measurements, J. Acoust. Soc. Am. 60 (4) (1976) 848{856.

[23] W. A. Kinney, A. D. Pierce, R. E. J., Helicopter noise experiments in an urban environment, J. Acoust. Soc. Am. 56 (2) (1974) 332{337.

[24] R. H. Lyon, R. G. DeJong, Theory and Application of Statistical Energy Analysis, Butterworth-Heinemann, 1995.

[25] M. E. Delany, E. N. Bazley, Monopole radiation in the presence of an absorbing plane, J. Sound Vib. 13 (3) (1970) 269{279.

[26] M. Gensane, F. Santon, Prediction of sound elds in rooms of arbitrary shape: validity of the image sources method, J. Sound Vib. 63 (1) (1979) 97{108.

[27] U. Ingard, On the re ection of a spherical sound wave from an in nite plane, J. Acoust. Soc. Am. 23 (3) (1951) 329{335.

[28] M. A. Nobile, S. I. Hayek, Acoustic propagation over an impedance plane, J. Acoust. Soc. Am. 78 (4) (1985) 1325{1336.

[29] H. Shirai, L. B. Felsen, Rays, modes and beams for plane wave coupling into a wide open-ended parallel-plane waveguide, Wave Motion 9 (2) (1987) 301{317.

[30] H. Y. Yee, L. B. Felsen, J. B. Keller, Ray theory of re ection from the open end of a waveguide, SIAM J. App. Math. 16 (2) (1968) 268{300.

[31] B. van der Pol, H. Bremmer, Operational Calculus based on the two-sided Laplace Integral, Cambridge University Press, 1950.

[32] E. J. Watson, In nite regular electrical networks, Eur. J. Appl. Math. 16 (5) (2005) 555{567.